The Insights of Lithium Metal Plating/Stripping in Porous Hosts: Progress and Perspectives

Ying-Xin Zhan, Peng Shi, Xue-Qiang Zhang, Fei Ding, Jia-Qi Huang,* Zhehui Jin, Rong Xiang, Xingjiang Liu,* and Qiang Zhang*

Lithium (Li) metal is strongly regarded as a promising anode for next-generation secondary batteries. However, the nonuniform plating/stripping and volume fluctuation of the Li metal anode give rise to low Coulombic efficiency and short lifespan of Li metal batteries, which hinder practical applications of the Li metal anode. A composite Li metal anode that employs a stable porous host has been proposed as a promising strategy to regulate the behaviors of Li plating/stripping and relieve volume fluctuation. In a porous host, the basic building block is a pore. The pore structure affects the distribution of electric and Li-ion concentration fields during Li plating/stripping, thus regulating Li plating/stripping and the lifespan of the composite Li metal anode. Therefore, herein, the recent progress in investigating the behavior of Li plating/stripping in a pore based on liquid electrolytes is summarized from the aspects of pore diameter, depth, and tortuosity. Furthermore, the perspectives of rational design of the pore structure for a composite Li metal anode are presented to promote the development of Li metal anodes.

1. Introduction

The increasing applications of electrical vehicles and portable electronic devices raise strong requirements for the development of high-energy-density rechargeable batteries.[1,2] However, the specific energy of commercialized lithium-ion batteries (LIBs) with a graphite anode is approaching the theoretical limit.[3,4] Therefore, lithium (Li) metal is reviving as the anode in high-energy-density rechargeable batteries due to its high theoretical specific capacity (3860 mA h g^{-1}) and low reduction potential (–3.04 V versus standard hydrogen electrode).[5–9] Moreover, Li metal anodes (LMAs) can be combined with different types of cathodes, such as sulfur,[10–16] oxygen,[17–19] and intercalation-type cathodes,[20–24] attracting intensive research attention and interest.

However, practical applications of LMAs are still hindered by the uncontrolled behavior of Li plating/stripping, generally termed "Li dendrites," and extreme volume fluctuation.[25–28] These severe drawbacks significantly reduce the lifespan of lithium metal batteries (LMBs) and even result in hazardous safety issues. To date, tremendous efforts have been devoted to developing strategies to address the drawbacks of LMAs, such as electrolyte engineering,[29–38] interface modification,[39–48] composite anodes,[49–55] theoretical simulations,[53,56–59] and so on.[60] Therein, the composite Li anode that combines a porous host with Li metal has emerged as a promising candidate to circumvent the issues of planar Li metal as an anode.

The porous host in a composite Li anode can regulate the behavior of Li plating/stripping and relieve the volume fluctuation to enhance the stability and lifespan of the LMA. First, the

Y.-X. Zhan, Prof. J.-Q. Huang
School of Materials Science and Engineering
Beijing Institute of Technology
Beijing 100081, China
E-mail: jqhuang@bit.edu.cn

Y.-X. Zhan, Prof. J.-Q. Huang
Advanced Research Institute of Multidisciplinary Science
Beijing Institute of Technology
Beijing 100081, China

P. Shi, X.-Q. Zhang, Prof. Q. Zhang
Beijing Key Laboratory of Green Chemical Reaction Engineering and Technology
Department of Chemical Engineering
Tsinghua University
Beijing 100084, China
E-mail: zhang-qiang@mails.tsinghua.edu.cn

Dr. F. Ding, Dr. X. Liu
Science and Technology on Power Sources Laboratory
Tianjin Institute of Power Sources
Tianjin 300384, China
E-mail: xjliu@nklps.org

Prof. Z. Jin
School of Mining and Petroleum Engineering
Department of Civil and Environmental Engineering
University of Alberta
Edmonton, AB T6G 1H9, Canada

Prof. R. Xiang
Department of Mechanical Engineering
The University of Tokyo
Tokyo 113-8656, Japan

porous host reduces the real current density for Li plating/stripping by increasing the specific surface area, which contributes to uniform Li deposition according to the model of Sand's time.[61,62] Second, the modification of surface properties of a porous host can guide Li plating into a homogeneous form by polar functional groups,[63,64] alloy layers,[28,65] and so on. Third, the porous host can accommodate the deposited Li inside to maintain dimensional stability compared to the extreme volume change of hostless LMAs.[66,67] Generally, the basic building block of a porous host is a pore, where the plating/stripping of Li occurs originally. The distribution of electric and Li-ion concentration fields as the necessary conditions for electrochemical plating/stripping is significantly impacted by the pore structure. The behavior of Li plating/stripping in each pore jointly dictates the whole utilization efficiency and the lifespan of an LMA. Therefore, the insights of Li plating/stripping in a pore of the porous host not only provide fundamental understanding to disclose the role of a porous host in current composite Li anodes, but also offer rational guidance to further design a specific porous host for practical composite Li anodes.

Porous hosts with different pore structures have been developed to investigate and regulate the behaviors of Li plating/stripping for working LMAs. However, discussions of the pore structure are qualitative and even vague in most publications, which is not conducive to further rational design. Moreover, the understanding of the relation between the pore structure and the behaviors of Li plating/stripping in a porous host is critical and should be emphasized for promoting the process of composite Li anodes.

In this review, the behaviors of Li plating/stripping in porous hosts are summarized from the aspects of pore structure. This review focuses on the pore structure in conductive and porous hosts based on liquid electrolytes. The topic related to the pore in nonconductive hosts and solid-state electrolytes is discussed in other impactful publications.[50,51,68,69] The pore structure of the host is quantitatively described based on the pore diameter, depth, and tortuosity (**Figure 1**). The recent progress in designing and investigating the pore structure of a host for a composite Li anode is summarized and the merits and limitations of different pore structures are pointed out. In addition, the morphology evolution of deposited Li in typical examples of pore structure are sorted. The relations between the pore structure and the

behaviors of Li plating/stripping Li are discussed. The Coulombic efficiency (CE) and lifespan of the porous structure hosts with the different pore structures described in this review are partially summarized in **Table 1**. Finally, the perspectives of rational design of the pore structure for composite Li anodes are further proposed to facilitate the development of LMBs.

2. Pore Diameter

The pore diameter significantly impacts the distribution of electric and Li-ion concentration fields of a pore before and after a cycle, especially near the mouth of a pore. The distribution of electric and Li-ion concentration fields near the mouth of a pore is the precondition for Li plating/stripping inside the pore. Moreover, the pore diameter is also a significant factor in the specific surface area for a porous host. Typical examples of different pores are shown in **Figure 2**, which are very different from the range of materials, especially for nanomaterials. The diameter of a pore in porous hosts for composite Li anodes ranges from nanometers to tens of micrometers. Therefore, the diameter of a pore can be divided into three types according to the investigated porous hosts for composite Li anodes: small ($<1\,\mu m$), medium (1–$10\,\mu m$), and large ($>10\,\mu m$).

2.1. Small Pore

The research of the distribution of electric and Li-ion concentration fields of a small pore is insufficient and further investigations are highly required. Generally, the transport length of an ion will diminish with decreasing diameter of a pore. In addition, a small pore contributes to a higher specific surface area than medium and large pores for a porous host, and thus decreases the areal current density more obviously. Porous carbon hosts with small pores, such as carbon nanotubes (CNTs) and graphene, are generally used due to their high conductivity, light weight, and good electrochemical and mechanical stability.

A solid electrolyte interphase coated graphene (SCG) host with a small pore of $\approx10\,nm$ to regulate the behavior of Li plating was demonstrated by Zhang and co-workers.[70] The abundant unblocked ion pathways and high electron conductivity of a small
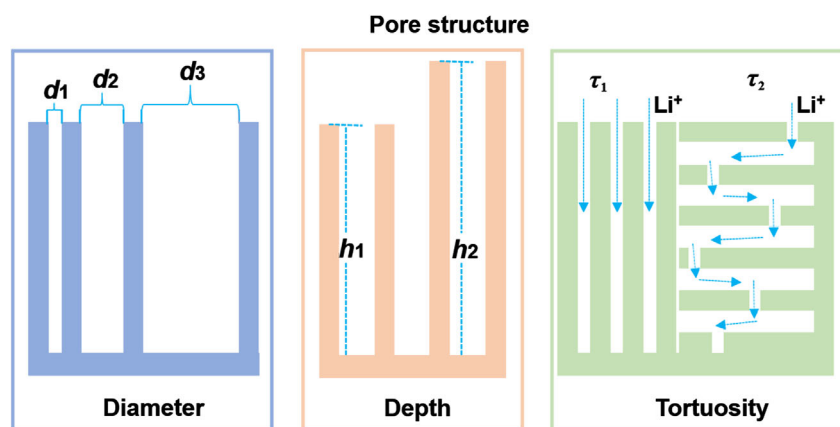

Figure 1. Three factors of pore structure: diameter, depth, and tortuosity.

Table 1. The CE and lifespan of porous hosts based on different pore structures.

Pore structure		Host materials	Current density and cycling capacity [mA cm^{-2}/mA h cm^{-2}]	CE [%]/cycle number	Ref.
	Small pore (<1 μm)	SEI-coated graphene	0.5/0.5	97/100	[70]
Pore diameter		Unstacked graphene	2/1	93/50	[71]
		C-host@Cu	1/1	99/250	[72]
		CNT sponge	1/2	98.5/90	[73]
		CMK-3	1/1	95/200	[74]
	Medium pore (1–10 μm)	3D current collector	1/1	97/140	[75]
		3D CuNW	1/1	98.6/200	[78]
		3D-AGBN	1/6	97.3/50	[80]
		TiC/C	1/1	98.5/100	[81]
	Large pore (10 μm)	3D hollow carbon fiber	2/4	99/90	[82]
		3DP-Cu	1/5	95.5/53	[102]
		Copper mesh	0.5/1	97/70	[100]
		3DP-NC	1/10	97.9/100	[103]
Pore depth	50 μm	Cu-5-50-12	1/3	98.5/200	[86]
	40 μm	2h-3D CuZn	1/1	95/150	[87]
Pore tortuosity	4.46	Horizontally aligned rGO aerogel	1/1	96.7/120	[94]
	1.25	Vertically aligned rGO aerogel	1/1	99.1/300	[94]

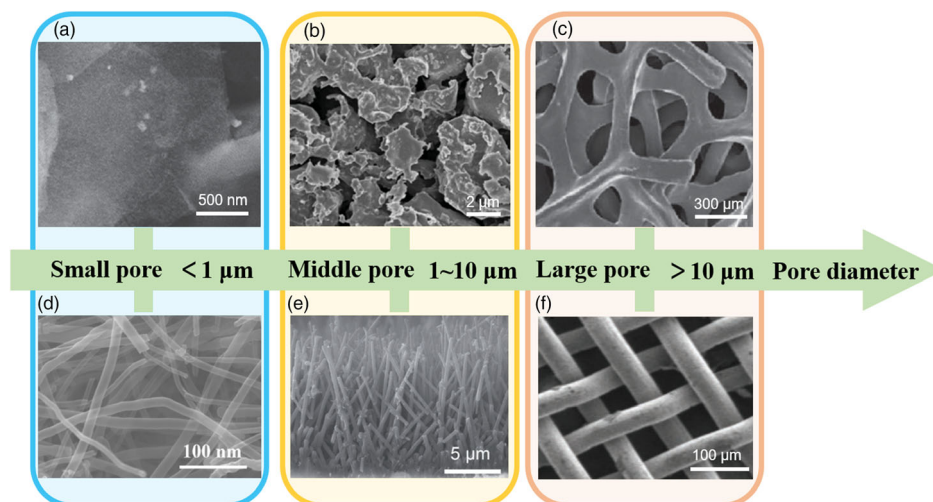Small pore < 1 μm   Middle pore 1~10 μm   Large pore > 10 μm   Pore diameter

Figure 2. The SEM images of typical examples of the host with different pore diameters. a) SEM images of graphene. Reproduced with permission.[71] Copyright 2016, Wiley-VCH. b) SEM images of brass tapes after chemical dealloying. Reproduced with permission.[75] Copyright 2016, Wiley-VCH. c) SEM image of a commercial Cu foam. Reproduced with permission.[75] Copyright 2016, Wiley-VCH. d) SEM images of carbon nanofiber network. Reproduced with permission.[101] Copyright 2016, Springer Nature. e) SEM images of TiC/C nanowires arrays. Reproduced with permission.[81] Copyright 2017, Wiley-VCH. f) SEM images of copper mesh. Reproduced with permission.[100] Copyright 2017, Wiley-VCH.

pore in the graphene host afford the fast transfer of Li ions and thus the composite anode possesses a high ionic conductivity. Li can be deposited in the small pore of interspace graphene, effectively restraining volume expansion. The composite anode can achieve a high CE of 93% at a current density of 2.0 mA cm^{-2}. The unstacked graphene with extensive small pores (0–10 nm) has a larger specific surface area (1666 m^2 g^{-1}) and thus an extremely low local current density is achieved (**Figure 3**a).[71]

The sandwich-like core–shell structure of the anode enables LMBs to maintain a stable cycle and a high CE of 93% at a cycling capacity of 5.0 mA h cm^{-2} and a current density of 2.0 mA cm^{-2}. In addition to graphene, a porous CNT sponge on Cu foil was directly prepared by Gui et al. (Figure 3b).[72] The CNT sponge has high porosity to store enough Li and accommodate huge volume fluctuation. The Li deposition is well bound to the CNT and is mainly stored inside the CNT sponge instead of on
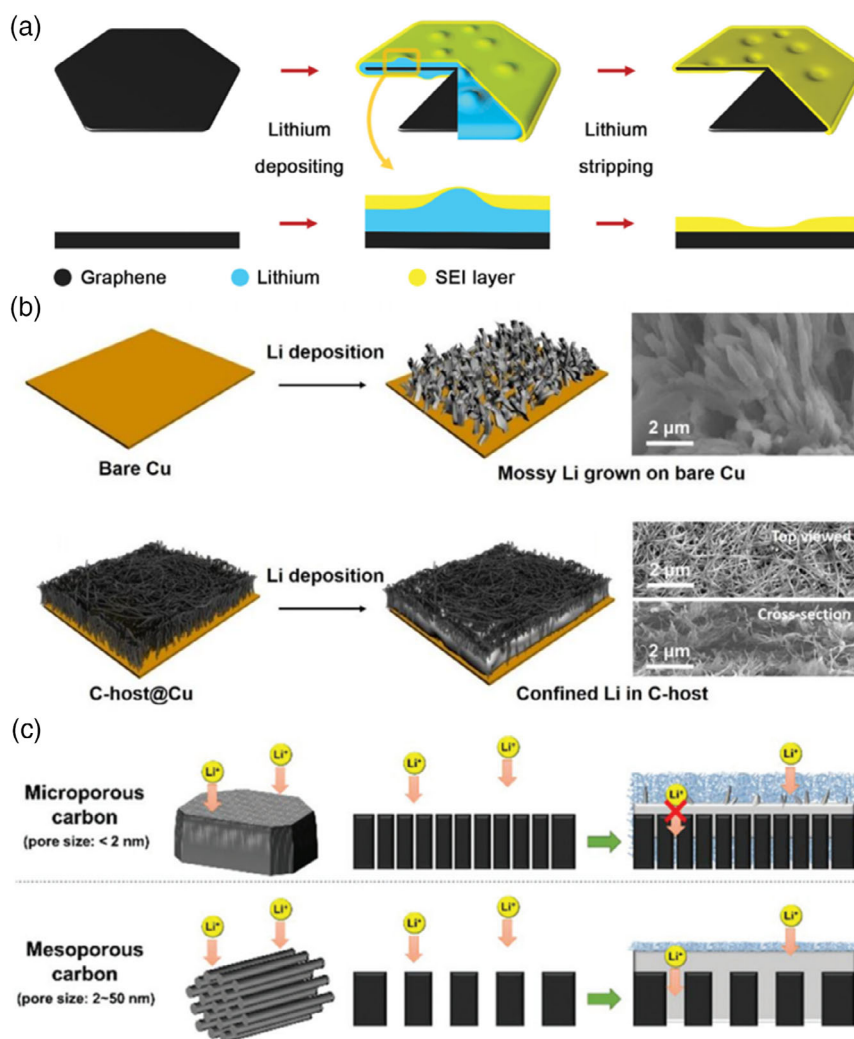
Figure 3. Porous hosts with a small pore. a) Schematic diagrams of Li plating/stripping behavior on a graphene flake. Reproduced with permission.[71] Copyright 2016, Wiley-VCH. b) Morphology comparison of Li deposition on bare Cu and C-host@Cu. Reproduced with permission.[72] Copyright 2018, Elsevier. c) Schematic of the effect of a nanoporous carbon host on Li plating. Reproduced with permission.[74] Copyright 2020, Royal Society of Chemistry.

the surface, thus restraining the growth of Li dendrites. Moreover, a prelithiated CNT sponge with much higher chemical affinity with Li metal was presented by Wang and co-workers.[73] The pore diameter of the CNT sponge is 1–100 nm. The CNT sponge has a reversible Li storage capacity of 150 mA h g^{-1} above 0.0 V and the large specific surface area and lithiophilicity lead to a reduced nucleation overpotential. It was demonstrated that the CNT sponge is favorable for depositing Li without dendrites with an ultrahigh capacity of 10.0 mA h cm^{-2}.

Recently, the effects of the pore diameter of nanoporous carbon on stabilizing the LMAs were evaluated by Jo et al. (Figure 3c).[74] Microporous carbon (MSP-20, <2 nm) and mesoporous carbon (CMK-3, 3.4 nm) were selected as porous hosts. The microporous carbon with large specific surface area can extend the Sand's time compared to the mesoporous carbon. Sand's time defines the initiation time of the formation of Li dendrites theoretically and extension of the Sand's time indicates

that the formation of Li dendrites is postponed or even inhibited, which contributes to stable plating/stripping of the LMA. However, the micropores are easily clogged due to the decomposition of the electrolyte to restrict the diffusion of Li ions into micropores. The mesopores maintain the accessibility of Li ions and afford abundant space for Li plating/stripping. The mesoporous carbon confines Li metal better and affords a much more increased lifespan than the microporous carbon. The CE of the cell with CMK-3 was over 95% within 200 cycles; however, the CE was only 90% in the cell with MSP-20 during 80 cycles under 1.0 mA cm^{-2} for 1 h.

The small-pore host exhibits great potential and advantage in regulating the Li plating/stripping process. However, smaller is not always better. The side issues induced by a small pore should be considered. 1) The high specific surface area with a small pore decreases the local current density. However, the high surface area remarkably increases the contact area between the

electrolyte and Li metal. Thus, a solid electrolyte interphase (SEI) forms and results in tremendous consumption of the electrolyte. Furthermore, the access of ion diffusion can be clogged during subsequent cycles due to the accumulation of the SEI. In addition to SEI, small pores can be easily clogged by dead Li, and the active surface area of blocked pores cannot be fully utilized. 2) Hosts with small pores are hardly free-standing and must be combined with current collectors, increasing the contact resistance and the complexity of the composite Li anode. 3) The common fabrication method of composite Li anodes with a small-pore host is molten Li infusion, which requires harsh operating conditions. The risk and cost should be evaluated when it comes to scale-up preparation. Therefore, hosts with small pores are excellent for proof of concept in research of the behavior of Li plating/stripping; however, the practical potential needs to be further explored.

2.2. Medium Pore

Compared to hosts with a small pore, medium-pore hosts are elaborately designed to promote practical applications of LMBs. A medium-pore host prepared by the chemical dealloying method was fabricated by He et al.[75] The pore diameter can be easily tuned by adjusting the dealloying time. The pore structure can provide a large inner surface area and space to accommodate deposited Li. The host with medium pores (1–2 μm) exhibits the best performance in full cells. The CE of the host maintained at 97% for nearly 140 cycles at $1.0\,mA\,cm^{-2}$ for 1 h. However, it is difficult to achieve uniform pore diameter by the chemical dealloying process. A compact porous Cu host with uniform pore diameter was produced by a novel electrochemical etching method (**Figure 4**a).[76] The uniform medium pore of ≈1 μm enables a small local current density and slows down the consumption of the electrolyte compared to small pores, resulting in uniform Li plating/striping inside pores and long cycle numbers.

In addition to alloys as original materials to prepare porous hosts, Yao et al. designed a free-standing Cu host (Figure 4b).[77] Due to the opened medium pores (1–5 μm) of the free-standing Cu nanowires (CuNWs), Li metal can fill the pores to form a CuNW-reinforced composite Li anode. Under the current density of $1.0\,mA\,cm^{-2}$, up to $7.5\,mA\,h\,cm^{-2}$ of Li can be plated into the CuNW host without the growth of Li
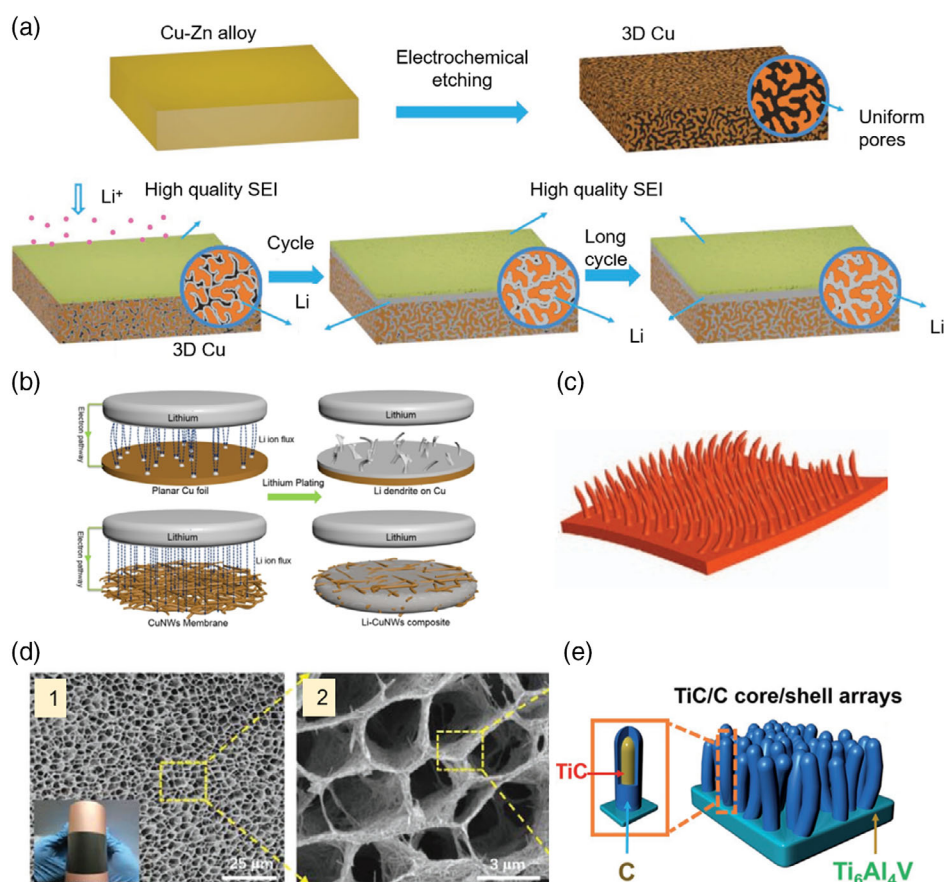

Figure 4. A porous host with a medium pore. a) Schematic of fabrication of 3D Cu host and Li plating on the host during cycling. Reproduced with permission.[76] Copyright 2018, Wiley-VCH. b) Schematic of Li ion flux distribution and Li metal plating models on planar Cu foil and CuNW host. Reproduced with permission.[77] Copyright 2016, American Chemical Society. c) Schematic presentation of the 3D porous Cu. Reproduced under the terms of the CC-BY 4.0 license.[79] Copyright 2015, The Authors, published by Springer Nature. d) SEM images of the optimized 3D-AGBN host with hierarchical binary structure. Reproduced with permission.[80] Copyright 2018, Wiley-VCH. e) Schematic diagram for the TiC/C host. Reproduced with permission.[81] Copyright 2018, Wiley-VCH.

dendrites. The CuNWs can perform for 200 cycles and the average CE of the host can be up to 98.6% at the current density of 1.0 mA cm^{-2}.[78] In addition, a 3D Cu current collector with a medium pore diameter of 2.1 μm was explored by Guo and co-workers, where Li can be reversibly plated/stripped from the host with a high CE of 98.5% (Figure 4c).[79] The medium pore of the 3D Cu host affords a high pore volume to accommodate the Li metal with an appropriate capacity. Moreover, a silver nanowire and graphene-based hierarchical host (3D-AGBN) was designed by Xue et al. for a composite Li anode (Figure 4d).[80] The average pore diameter of the host is ≈3 μm. The porous interconnection structure, with great mechanical strength and electrochemical stability, can support grand deposited Li and keep the electrode volume constant during ultrafast cycling. Therefore, the CE of the 3D-AGBN maintained at 97.3% within 50 cycles under the current density of 1.0 mA cm^{-2} with the cycling capacity of 6.0 mA h cm^{-2}.

Meanwhile, a variety of inorganic nonmetallic hosts with medium pores can be conveniently prepared by chemical vapor deposition and self-assembly. A self-supporting TiC/C core/shell nanowire host with a medium pore (1–2 μm) was reported by Liu et al. (Figure 4e).[81] When the TiC/C host with medium pore was introduced to accommodate deposited Li, the streamlines of the electric field exhibited uniform distribution, which effectively homogenized the Li ion distribution and shielded any electric field perturbations for Li plating. The CE of the TiC/C host could maintain around 98.5% for 100 cycles with a cycling capacity of 1.0 mA h cm^{-2} at 1.0 mA cm^{-2}.

Despite the advantages of a medium pore in a porous host, the potential issues cannot be ignored. 1) The pore diameters of most of the medium-pore hosts reported earlier are not uniform; therefore, it is difficult to determine the most suitable pore diameter for Li plating/stripping. It is still a challenge to precisely control the uniform pore diameter of the porous host. 2) Most medium-pore hosts are based on metal materials that are much denser than Li metal, such as alloys and metal nanowires. The mass of the host should be further reduced to satisfy the requirements of energy density of practical batteries. 3) Modifications of lithiophilic materials inside the medium pore are required to enhance the wettability of the host to fabricate the composite anode and guide the deposition of Li metal.

2.3. Large Pore

A host with a large pore has a huge inside space, which provides enough room for a large amount of Li deposition. A free-standing hollow carbon fiber (CF) host with high specific surface area was demonstrated by Guo et al., which can significantly decrease the local current density and improve the Li plating/stripping behavior (**Figure 5**a).[82] Li is confined to the large pore (10–50 μm) between fibers. Therefore, the CE achieved was 99% for 90 cycles with a capacity of 4.0 mA h cm^{-2} and 99% for 75 cycles with an even higher capacity of 6.0 mA h cm^{-2}. In addition, a freestanding graphitized CF host was reported by Wu et al., which can bear an ultrahigh areal capacity of 8.0 mA h cm^{-2} (Figure 5b).[83] The pore diameter of the host is 72 μm on average based on mercury porosimetry analysis, which mainly comes from the voids between CFs. The large

interconnected pores effectively ameliorate the infinite volume expansion during Li plating/stripping. Furthermore, Shi et al. directly obtained a Li/carbon fiber (Li/CF) Li-containing composite anode by a one-step rolling method (Figure 5c).[84] As the CF host affords abundant large pores (30–60 μm) to accommodate Li metal, the Li/CF anode can provide a large specific capacity of up to 1841 mA h g^{-1}. Thus, the Li/CF | S pouch cell displayed a large discharge capacity of 3.25 mA h cm^{-2} and the capacity retention rate was over 98% at 0.1 C after 100 cycles.

Conductive hosts with large pores are also used to accommodate the high capacity of deposited Li apart from CFs. A stainless-steel fibrous felt was introduced by Kim and co-workers to enable the compaction of a porous Li layer in the large pores (10–200 μm) between the metal fibers.[85] Moreover, it can guide the reversed growth of the deposited Li toward the inside of the host (Figure 5d). The stainless-steel fibrous-felt composite LMA exhibited stable cycling at 10.0 mA cm^{-2} for more than 100 cycles with a small overpotential of 30 mV.

In a summary, a host with large pores can accommodate massive deposition of Li metal. The moderate specific surface area by large pores decreases the consumption of the electrolyte compared to small and medium pores. Moreover, composite Li anodes with large-pore hosts can be prepared by the roll-in method, which is more appropriate for practical conditions and large-scale fabrication compared to molten Li infusion and electrodeposition methods. However, the ability to confine the deposited Li in the pores decreases with increasing pore diameter. When the pore diameter is close to the macroscale, the specific surface area of the host has no order-of-magnitude change compared to the planar current collector, thus losing the effects of space constraint and dendrite suppression. Li metal can easily detach from the host fiber, resulting in electric disconnection and low CE. Therefore, the pore diameter of a host should be designed in a reasonable range according to actual application requirements.

3. Pore Depth

In addition to the pore diameter, the pore depth is another important parameter to determine the specific surface area and pore volume. Moreover, the pore depth has a significant effect on the electric field distribution of the host according to the quantitative results of the phase field model (**Figure 6**a).[58] When a channel length (pore depth) increases from 50 to 150 μm at a fixed width (pore diameter), the current density increases from 70.4 to 160.1 mA cm^{-2}, which has a different regulation against that with different pore diameters.

The regulations of Li plating/stripping behaviors in porous Cu with different pore depths were explored by Guo and co-workers (Figure 6b).[86] The morphology of deposited Li is diverse on the porous Cu when the pore depth of the host is 50, 30, and 25 μm, respectively. The initial spherical deposited Li changes into a shuttle-shaped morphology when the pore depth decreases from 50 to 30 μm, and the diameter of the deposited Li increases significantly. More deposited Li is formed on the surface of porous Cu and the diameter of the deposited Li rapidly increases to 30 μm when the pore depth is 25 μm. The different morphologies of deposited Li are attributed to the change of the current distribution and the decreased specific surface area. The CE of the
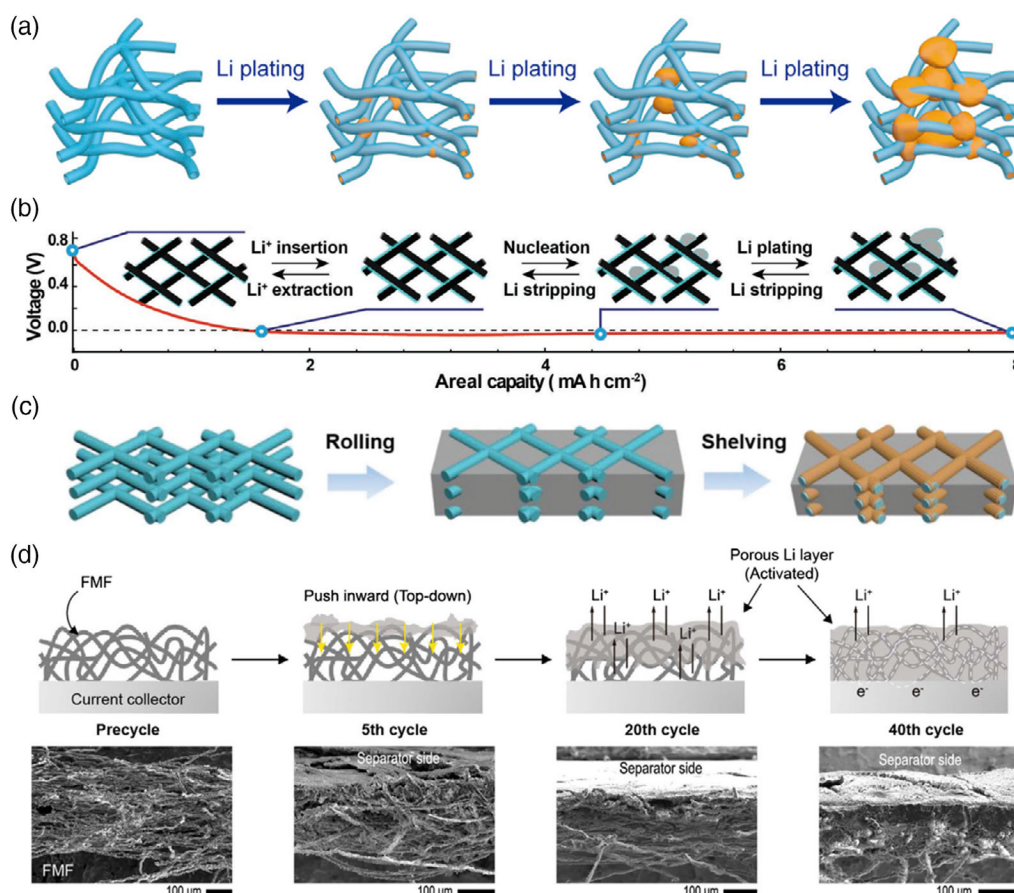
**ADVANCED
SCIENCE NEWS**
www.advancedsciencenews.com

Energy Technology
Generation, Conversion, Storage, Distribution
www.entechnol.de

Figure 5. A porous host with a large pore. a) Schematic of Li deposition behavior on 3D hollow CF. Reproduced with permission.[82] Copyright 2017, Elsevier. b) Illustration of the plating/stripping process of the graphitized CF electrode. Reproduced with permission.[83] Copyright 2017, Wiley-VCH. c) Preparation of a Li/CF composite anode with large pores. Reproduced with permission.[84] Copyright 2019, Wiley-VCH. d) The morphological evolution of fibrous metal felt electrodes during a half-cell test. Reproduced under the terms of the CC-BY 4.0 license.[85] Copyright 2016, The Authors, published by Springer Nature.

porous Cu with a pore depth of 50 μm can maintain around 98.5% for 200 cycles with a cycling capacity of 3.0 mA h cm^{-2} at 1.0 mA cm^{-2}. However, the porous Cu with a pore depth of 25 μm has poor cycling performance of 60 cycles. In addition, Lu et al. prepared a host with different pore depths by the dealloying method.[87] The depths of the porous host layers of 3D CuZn were ≈40, 80, and 100 μm, respectively (Figure 6c). The CE of 3D CuZn with a pore depth of 40 μm indicated a high retention of 95% for 150 cycles with a capacity of 1.0 mA h cm^{-2} at a current density of 1.0 mA cm^{-2}, whereas the hosts with pore depths of 80 and 100 μm exhibited low CEs that were less than 90% after 80 and 60 cycles, respectively. The smaller pore depth leads to improved CE for a longer lifespan and a lower plating/stripping overpotential. The improvement is mainly attributed to the presence of Li preferred nucleation sites in the porous host in the original report. However, the effect of the pore depth should be also taken into considerations.

With the increase of the pore depth, the host provides more space for deposited Li, ensuring minimized volume change even with a high deposition capacity. However, too deep a pore extends the transport path of Li ions and thus the resistance to deposition inside the host increases. Li ions will be preferred to deposit on the surface at the top of the host due to its high conductivity and low resistance. Therefore, the deposited Li in the host with a deep pore depth is uneven and most space inside the host cannot be utilized. To guide Li deposition from the bottom of the host, a gradient lithiophilic 3D conductive host was designed by Xie et al., in which the content of the lithiophilic element (Si) decreases from the bottom to the top gradually.[88] The gradient lithiophilic structure enables the Li metal to deposit first at the bottom, achieving high space utilization of the host with deep pore depth. Moreover, Hong et al. introduced a host with electric conductivity gradient for a LMA to suppress Li plating on the top surface and enabled stable cycling for more than 250 cycles at 1.0 mA cm^{-2}.[89] The simulation results proved that the local reaction flux of Li ions at the bottom layer is more concentrated than at the top layer.

In summary, pore depth is significantly related to the specific surface area and pore volume of a host and has a strong effect on the current distribution. Different pore depths of hosts will affect the deposition morphology of Li, thus changing the CE and cycle
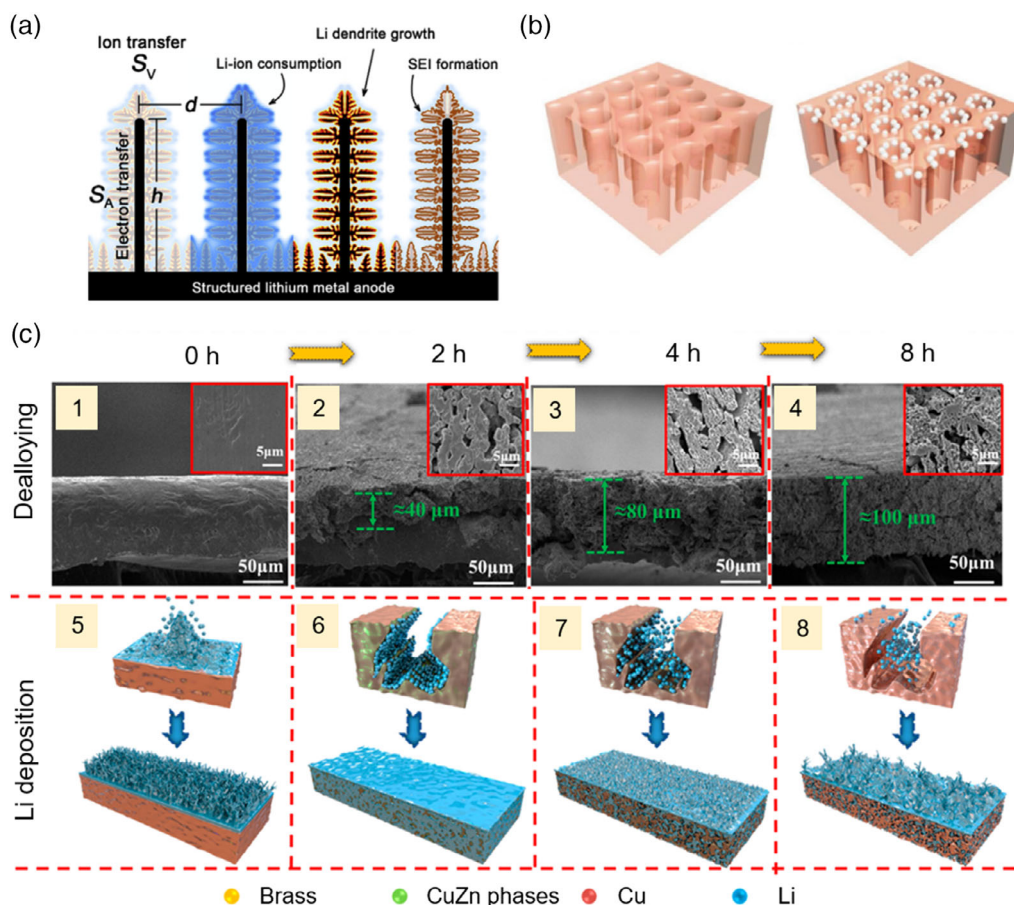
Figure 6. The insight of pore depth on Li deposition behavior. a) Schematic illustration of the simulated structured LMA. Reproduced with permission.[58] Copyright 2019, Elsevier. b) Schematic diagram for the designed porous Cu current collectors. Reproduced with permission.[86] Copyright 2017, Wiley-VCH. c) Li deposition diagram showing different current collectors after dealloying at 0, 2, 4, and 8 h. Reproduced with permission.[87] Copyright 2020, American Chemical Society.

life of the battery. A deeper pore provides much more space for deposited Li but it extends the transport path of Li ions in the host and increases the resistance of Li deposition at the bottom of the host. In contrast, a small pore depth leads to a short transport path of Li ions and a low plating/stripping overpotential, but the capacity of a small pore depth to accommodate deposited Li is limited. The pore depth of the host should be designed within a reasonable range according to different scenarios. The gradient host can guide Li deposition from the bottom to the top, improving the space utilization of the host. However, the gradient feature of a host may change with increasing cycle number and lose the originally designed effect. The practical potential of the gradient host should be further explored.

4. Pore Tortuosity

Tortuosity is an effective geometric parameter to describe the complexity of pore structure of a host. It is worth noting that the tortuosity of a traditional graphite anode is considered an important parameter, which seriously affects the concentration gradient of Li ions during fast charge. Similarly, the ionic

transport, liquid-phase diffusivity, and conductivity are affected by the tortuosity in composite LMAs.

$$K_{\text{eff}} = \frac{K\epsilon}{\tau} \tag{1}$$

$$D_{\text{eff}} = \frac{D\epsilon}{\tau} \tag{2}$$

where ϵ, τ, K_{eff}, and K are the porosity, tortuosity, and effective and intrinsic conductivities, respectively. D_{eff} and D are the effective and intrinsic diffusivities, respectively. "Intrinsic" represents the property of the pure electrolyte (filling 100% of the volume) and "effective" represents the measured property of the electrolyte when it is filled within a porous structure.[90,91] Equation (1) and (2) serve as the definition of tortuosity (τ) used in most of the literature.

A Li metal/carbonized wood (C-wood) composite anode with low tortuosity was fabricated by preinjection method (**Figure 7**a).[92] The uniform microchannels in the C-wood endow reduced tortuosity, which improves the electrolyte diffusion and shortens the Li-ion transport distance in the host. Due to the high porosity and low tortuosity of the C-wood structure, a
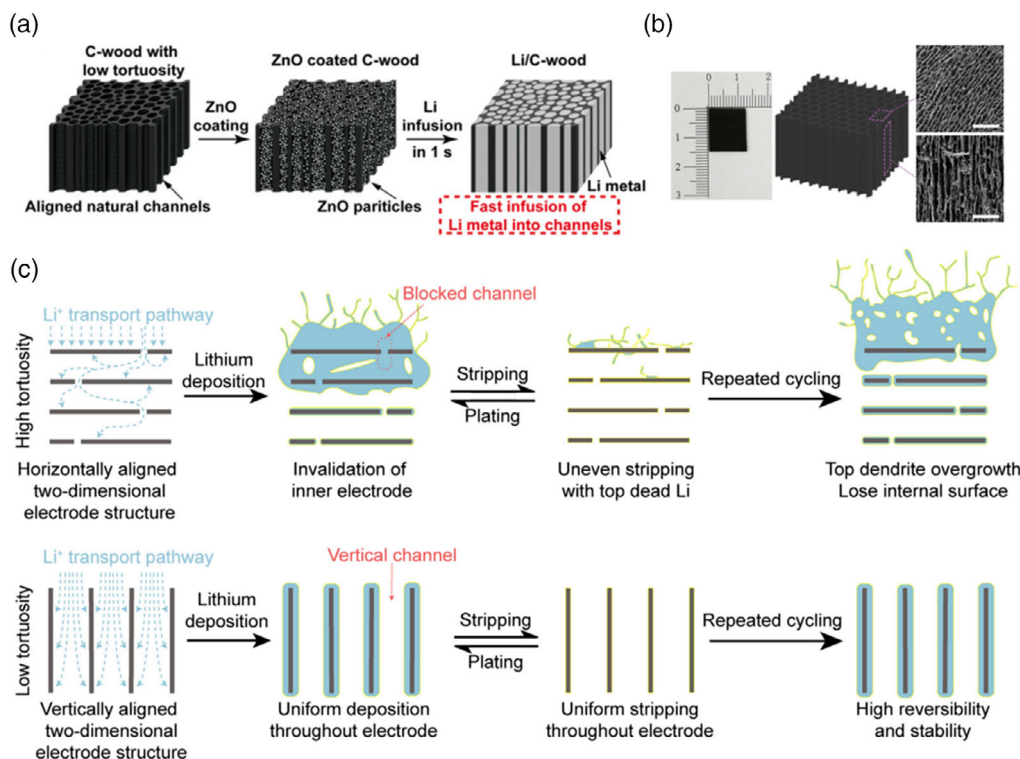
ADVANCED
SCIENCE NEWS
www.advancedsciencenews.com

Energy Technology
Generation, Conversion, Storage, Distribution

www.entechnol.de

Figure 7. A porous host with different tortuosity structures. a) Fabrication process of the Li/C-wood composite anode. Reproduced with permission.[92] Copyright 2017, National Academy of Sciences. b) Schematic of a typical carbon host with vertical channels. Reproduced with permission.[93] Copyright 2019, Oxford University Press. c) Schematic of the effect of tortuosity on the structure evolution of an LMA during cycling. Reproduced with permission.[94] Copyright 2020, Elsevier.

homogenous Li ion flux distribution is provided to enable uniform Li nucleation and growth. The expansion/contraction of the Li volume can be effectively accommodated within the natural channels of the C-wood, and the local current density can be further minimized due to the high porosity. Therefore, the low-tortuosity Li/C-wood host exhibited stable cycling for more than 225 cycles with a cycling capacity of $1.0 \, mA \, h \, cm^{-2}$ at $3.0 \, mA \, cm^{-2}$. Yao et al. reported a novel design of bioinspired low-tortuosity carbon with tunable vertical microchannels (Figure 7b).[93] The tunable vertical channels with low tortuosity can enable the rapid transport of Li ions, effectively mitigating the volume change of the anode during repeated Li stripping/plating. The low-tortuosity porous host with vertical channels enables fast charge transfer and rapid kinetics of electrochemical reactions. The vertical channels of the low-tortuosity host can still be observed after all Li has been stripped out, which indicates that this low-tortuosity structure can be well maintained during the Li stripping process. At the same time, the low-tortuosity vertical microchannels endow the host with a high specific surface area, lowering the practical areal current density, shortening the Li-ion transport path, and enabling uniform Li nucleation and growth in the host. The relationship between the pore diameter in the vertical channel and the electrochemical performance of the prepared Li composite anode was also disclosed. The smaller is the pore diameter of the vertical channel, the better the electrochemical performance.

In addition, the relationship between host tortuosity and cycling reversibility of composite Li anodes was first revealed by Cui and co-workers.[94] Li metal tends to plate and strip on the upper surface in a highly tortuous anode because the ion transport path to the middle or bottom of the host is much longer. The accumulation of deposited Li further impedes the ion transmission over time, thus aggravating the growth of excessive Li deposition on the top, while the surface inside the anode cannot be utilized effectively. During stripping, the residual dead Li accumulated on the upper surface further reduces the invertibility of the anode, blocks the path of ion inward transport, and aggravates the inhomogeneity of Li accumulation. On the contrary, a host with a low tortuosity enables Li ion to be uniformly transported and deposited in the host, which greatly improves the cycling stability (Figure 7c). The low-tortuosity host (1.25) achieved a high CE of 99.1% with a nearly identical overvoltage of 19 mV over 300 cycles with a cycling capacity of $1.0 \, mA \, h \, cm^{-2}$ at $1.0 \, mA \, cm^{-2}$. However, the high-tortuosity host (4.46) exhibited a low CE of 96.7% with a higher overpotential of 34 mV and decayed rapidly after 120 cycles at the same test conditions. Meanwhile, the simulation results prove that the lower tortuosity not only affords an obviously decreased Li ion concentration gradient near the anode, but also enables homogeneous current density distribution. A host with low pore tortuosity is appropriate for a composite Li anode. However, hosts with the same tortuosity have different effects on the behavior of Li plating/stripping due to differences in conductivity and lithiophilicity. Therefore, the design of tortuosity should be based on the selection of host materials.

5. Conclusion

To regulate behaviors of Li plating/stripping and relieve volume change, a composite Li anode that employs a stable porous host has been proposed as a promising strategy. Although porous hosts have achieved valuable progress in inhibiting Li dendrites and improving the cycling performance of LMAs, the fundamental understanding of the behavior of Li plating/stripping in a porous host is still insufficient to provide rational guidance for the design of composite Li anodes. The utilization efficiency and lifespan of a composite LMA are the apparent average result of the porous host instead of the basic reason why different porous hosts induce distinctive performance. In a porous host, the basic building block is a pore, and different pore sizes, depths, and tortuosities will lead to different transport pathways of Li ions, which strongly affects the distribution of electric and Li-ion concentration fields during Li plating/stripping, and the final performance of composite LMAs. To provide insights into the behavior of Li plating/stripping in a pore, the diameter, depth, and tortuosity of pore, three key parameters in description of the pore structure, have been investigated as summarized earlier. However, fundamental understanding of the behavior of Li plating/stripping is still scarce and more investigations are required for practical applications:

1) Model system and in situ characterization. It is difficult to obtain uniform and simple pore structure during the fabrication of a porous host. Thus, discussions of the pore structure are qualitative currently, which is not conducive to further understanding the Li plating/stripping behavior. To draw a clear and quantitative landscape of the effect of the pore diameter, depth, and tortuosity on the behavior of Li plating/stripping, simple and model systems with different materials in the range from several nanometers to tens of micrometers are highly required, which can be achieved by precision finishing and smart design. Meanwhile, in situ characterizations are necessary to record and analyze the behavior of Li plating/stripping.[95–97] 2) Theoretical simulations. The distribution of electric and Li-ion concentration field is difficult to detect by the experiments. Theoretical simulations, such as phase-field simulations,[98,99] can be used to quantitatively describe the change of electric and Li-ion concentration fields. Moreover, theoretical simulations can also describe the process of Li plating/stripping. 3) Li-containing composite anodes. Most studies on the effect of pore structure on the behavior of Li are based on a bare host without Li metal. However, Li-containing composite anodes, in which the pores are filled or half-filled by Li metal, are inevitable for practical applications when matching with different types of cathodes, especially for sulfur and oxygen cathodes. The effect of the pore structure on the behavior of Li plating/stripping should be further investigated based on Li-containing composite anodes. 4) The synergy of different pore structures. Generally, the reasonable design of the pore size is determined by the different purposes and application scenarios. A specific pore structure cannot possess all excellent properties and has limited ability to regulate the behavior of Li plating/stripping. The advantages of several pore structures can be effectively combined when it comes to practical applications. 5) Other properties. The pore structure depends on certain material. Therefore, the effect of the pore structure on the behavior of Li plating/stripping can change with the type of material. The other properties of a pore also should be considered, such as the electronic conductivity and the surface properties. Moreover, ingenious designing of other properties, such as gradient conductivity, can assist the improvement of the specific pore structure. However, the potential of these designs should be further evaluated under practical conditions. Furthermore, the decomposition of the electrolyte and the formation of SEI in a pore should be taken into consideration.

Porous hosts have produced remarkable improvements in understanding and regulating the behavior of Li plating/stripping, but they are still in the primary stage and face many challenges toward practical applications. The fundamental insights of the behavior of Li plating/stripping in a pore can provide rational guidance for the design of composite LMAs. Furthermore, investigations of the pore structure of composite Li anodes provide fresh insights and research methods for other advanced energy materials, such as sodium and potassium metal.

Conflict of Interest

The authors declare no conflict of interest.

[1] D. Larcher, J. M. Tarascon, *Nat. Chem.* **2015**, *7*, 19.
[2] H. D. Yoo, E. Markevich, G. Salitra, D. Sharon, D. Aurbach, *Mater. Today* **2014**, *17*, 110.
[3] Y. X. Lu, X. H. Rong, Y. S. Hu, L. Q. Chen, H. Li, *Energy Storage Mater.* **2019**, *23*, 144.
[4] T. Placke, R. Kloepsch, S. Dühnen, M. Winter, *J. Solid State Electrochem.* **2017**, *21*, 1939.
[5] Z. A. Ghazi, Z. Sun, C. Sun, F. Qi, B. An, F. Li, H. M. Cheng, *Small* **2019**, *15*, 1900687.
[6] H. Wang, D. Yu, C. Kuang, L. Cheng, W. Li, X. Feng, Z. Zhang, X. Zhang, Y. Zhang, *Chem* **2019**, *5*, 313.
[7] B. Liu, J. G. Zhang, W. Xu, *Joule* **2018**, *2*, 833.
[8] D.-H. Liu, Z. Bai, M. Li, A. Yu, D. Luo, W. Liu, L. Yang, J. Lu, K. Amine, Z. Chen, *Chem. Soc. Rev.* **2020**, *49*, 5407.
[9] K. Xu, *Energy Environ. Mater.* **2019**, *2*, 229.

[10] M. Zhao, B. Q. Li, X. Q. Zhang, J. Q. Huang, Q. Zhang, *ACS Cent. Sci.* **2020**, *6*, 1095.

[11] H. J. Peng, J. Q. Huang, X. B. Cheng, Q. Zhang, *Adv. Energy Mater.* **2017**, *7*, 1700260.

[12] W. Hua, Z. Yang, H. Nie, Z. Li, J. Yang, Z. Guo, C. Ruan, X. Chen, S. Huang, *ACS Nano* **2017**, *11*, 2209.

[13] Y.-X. Yao, X.-Q. Zhang, B.-Q. Li, C. Yan, P.-Y. Chen, J.-Q. Huang, Q. Zhang, *InfoMat* **2020**, *2*, 379.

[14] B.-Q. Li, L. Kong, C.-X. Zhao, Q. Jin, X. Chen, H.-J. Peng, J.-L. Qin, J.-X. Chen, H. Yuan, Q. Zhang, J.-Q. Huang, *InfoMat* **2019**, *1*, 533.

[15] S. Dörfler, H. Althues, P. Härtel, T. Abendroth, B. Schumm, S. Kaskel, *Joule* **2020**, *4*, 539.

[16] A. Manthiram, Y. Fu, S. H. Chung, C. Zu, Y. S. Su, *Chem. Rev.* **2014**, *114*, 11751.

[17] P. G. Bruce, S. A. Freunberger, L. J. Hardwick, J. M. Tarascon, *Nat. Mater.* **2011**, *11*, 19.

[18] C. Shu, J. Wang, J. Long, H. K. Liu, S. X. Dou, *Adv. Mater.* **2019**, *31*, 1804587.

[19] Y. Qiao, H. Deng, P. He, H. Zhou, *Joule* **2020**, *4*, 1445.

[20] X. Q. Zhang, C. Z. Zhao, J. Q. Huang, Q. Zhang, *Engineering* **2018**, *4*, 831.

[21] S. Chen, C. Niu, H. Lee, Q. Li, L. Yu, W. Xu, J.-G. Zhang, E. J. Dufek, M. S. Whittingham, S. Meng, J. Xiao, J. Liu, *Joule* **2019**, *3*, 1094.

[22] C. Niu, H. Lee, S. Chen, Q. Li, J. Du, W. Xu, J.-G. Zhang, M. S. Whittingham, J. Xiao, J. Liu, *Nat. Energy* **2019**, *4*, 551.

[23] R. Weber, M. Genovese, A. J. Louli, S. Hames, C. Martin, I. G. Hill, J. R. Dahn, *Nat. Energy* **2019**, *4*, 683.

[24] W. Zhang, Q. Wu, J. Huang, L. Fan, Z. Shen, Y. He, Q. Feng, G. Zhu, Y. Lu, *Adv. Mater.* **2020**, *32*, 2001740.

[25] X. B. Cheng, R. Zhang, C. Z. Zhao, Q. Zhang, *Chem. Rev.* **2017**, *117*, 10403.

[26] R. H. Wang, W. S. Cui, F. L. Chu, F. X. Wu, *J. Energy Chem.* **2020**, *48*, 145.

[27] L. Kong, Q. Jin, J. Q. Huang, L. D. Zhao, P. Li, B. Q. Li, H. J. Peng, X. T. Zhang, Q. Zhang, *Energy Technol.* **2019**, *7*, 1900111.

[28] C. Jin, O. Sheng, Y. Lu, J. Luo, H. Yuan, W. Zhang, H. Huang, Y. Gan, Y. Xia, C. Liang, J. Zhang, X. Tao, *Nano Energy* **2018**, *45*, 203.

[29] J. Qian, W. A. Henderson, W. Xu, P. Bhattacharya, M. Engelhard, O. Borodin, J. G. Zhang, *Nat. Commun.* **2015**, *6*, 6362.

[30] S. Chen, J. Zheng, D. Mei, K. S. Han, M. H. Engelhard, W. Zhao, W. Xu, J. Liu, J. G. Zhang, *Adv. Mater.* **2018**, *30*, 1706102.

[31] X. Q. Zhang, T. Li, B. Q. Li, R. Zhang, P. Shi, C. Yan, J. Q. Huang, Q. Zhang, *Angew. Chem., Int. Ed.* **2020**, *59*, 3252.

[32] X. Fan, L. Chen, O. Borodin, X. Ji, J. Chen, S. Hou, T. Deng, J. Zheng, C. Yang, S. C. Liou, K. Amine, K. Xu, C. Wang, *Nat. Nanotechnol.* **2018**, *13*, 715.

[33] X. Cao, X. Ren, L. Zou, M. H. Engelhard, W. Huang, H. Wang, B. E. Matthews, H. Lee, C. Niu, B. W. Arey, Y. Cui, C. Wang, J. Xiao, J. Liu, W. Xu, J.-G. Zhang, *Nat. Energy* **2019**, *4*, 796.

[34] Y. Ma, Z. Zhou, C. Li, L. Wang, Y. Wang, X. Cheng, P. Zuo, C. Du, H. Huo, Y. Gao, G. Yin, *Energy Storage Mater.* **2018**, *11*, 197.

[35] Y. Jie, X. Ren, R. Cao, W. Cai, S. Jiao, *Adv. Funct. Mater.* **2020**, *30*, 1910777.

[36] Y. Yamada, J. Wang, S. Ko, E. Watanabe, A. Yamada, *Nat. Energy* **2019**, *4*, 269.

[37] X. Wu, K. Pan, M. Jia, Y. Ren, H. He, L. Zhang, S. Zhang, *Green Energy Environ.* **2019**, *4*, 360.

[38] K. Xu, *Chem. Rev.* **2014**, *114*, 11503.

[39] R. Xu, Y. Xiao, R. Zhang, X. B. Cheng, C. Z. Zhao, X. Q. Zhang, C. Yan, Q. Zhang, J. Q. Huang, *Adv. Mater.* **2019**, *31*, 1808392.

[40] Q. Zhao, Z. Tu, S. Wei, K. Zhang, S. Choudhury, X. Liu, L. A. Archer, *Angew. Chem., Int. Ed.* **2018**, *57*, 992.

[41] Z. Lu, W. Li, Y. Long, J. Liang, Q. Liang, S. Wu, Y. Tao, Z. Weng, W. Lv, Q.-H. Yang, *Adv. Funct. Mater.* **2020**, *30*, 1907343.

[42] N. W. Li, Y. Shi, Y. X. Yin, X. X. Zeng, J. Y. Li, C. J. Li, L. J. Wan, R. Wen, Y. G. Guo, *Angew. Chem., Int. Ed.* **2018**, *57*, 1505.

[43] C.-Z. Zhao, H. Duan, J.-Q. Huang, J. Zhang, Q. Zhang, Y.-G. Guo, L.-J. Wan, *Sci. China Chem.* **2019**, *62*, 1286.

[44] C. Yan, H. Yuan, H. S. Park, J.-Q. Huang, *J. Energy Chem.* **2020**, *47*, 217.

[45] X.-Q. Zhang, X.-M. Wang, B.-Q. Li, P. Shi, J.-Q. Huang, A. Chen, Q. Zhang, *J. Mater. Chem. A* **2020**, *8*, 4283.

[46] Z. Hou, J. Zhang, W. Wang, Q. Chen, B. Li, C. Li, *J. Energy Chem.* **2020**, *45*, 7.

[47] Y. Zhao, G. Li, Y. Gao, D. Wang, Q. Huang, D. Wang, *ACS Energy Lett.* **2019**, *4*, 1271.

[48] Y. X. Yuan, F. Wu, G. H. Chen, Y. Bai, C. Wu, *J. Energy Chem.* **2019**, *37*, 197.

[49] H. Ye, Y. Zhang, Y. X. Yin, F. F. Cao, Y. G. Guo, *ACS Cent. Sci.* **2020**, *6*, 661.

[50] R. Zhang, N. W. Li, X. B. Cheng, Y. X. Yin, Q. Zhang, Y. G. Guo, *Adv. Sci.* **2017**, *4*, 1600445.

[51] P. Shi, X. Q. Zhang, X. Shen, R. Zhang, H. Liu, Q. Zhang, *Adv. Mater. Technol.* **2020**, *5*, 1900806.

[52] X. Shen, X. Cheng, P. Shi, J. Huang, X. Zhang, C. Yan, T. Li, Q. Zhang, *J. Energy Chem.* **2019**, *37*, 29.

[53] X. Chen, X. R. Chen, T. Z. Hou, B. Q. Li, X. B. Cheng, R. Zhang, Q. Zhang, *Sci. Adv.* **2019**, *5*, eaau7728.

[54] T. Li, P. Shi, R. Zhang, H. Liu, X. B. Cheng, Q. Zhang, *Nano Res.* **2019**, *12*, 2224.

[55] H. Ye, Z. J. Zheng, H. R. Yao, S. C. Liu, T. T. Zuo, X. W. Wu, Y. X. Yin, N. W. Li, J. J. Gu, F. F. Cao, Y. G. Guo, *Angew. Chem., Int. Ed.* **2019**, *58*, 1094.

[56] X. Chen, H. R. Li, X. Shen, Q. Zhang, *Angew. Chem., Int. Ed.* **2018**, *57*, 16643.

[57] O. Borodin, X. Ren, J. Vatamanu, A. von Wald Cresce, J. Knap, K. Xu, *Acc. Chem. Res.* **2017**, *50*, 2886.

[58] R. Zhang, X. Shen, X.-B. Cheng, Q. Zhang, *Energy Storage Mater.* **2019**, *23*, 556.

[59] Y. C. Fan, T. S. Wang, D. Legut, Q. F. Zhang, *J. Energy Chem.* **2019**, *39*, 160.

[60] X. L. Xu, S. J. Wang, H. Wang, C. Hu, Y. Jin, J. B. Liu, H. Yan, *J. Energy Chem.* **2018**, *27*, 513.

[61] J. Chazalviel, *Phys. Rev. A* **1990**, *42*, 7355.

[62] C. Brissot, M. Rosso, J. N. Chazalviel, S. Lascaud, *J. Power Sources* **1999**, *81–82*, 925.

[63] B.-Q. Li, X.-R. Chen, X. Chen, C.-X. Zhao, R. Zhang, X.-B. Cheng, Q. Zhang, *Research* **2019**, *2019*, 1.

[64] J. Lopez, A. Pei, J. Y. Oh, G. N. Wang, Y. Cui, Z. Bao, *J. Am. Chem. Soc.* **2018**, *140*, 11735.

[65] Q. Pang, X. Liang, I. R. Kochetkov, P. Hartmann, L. F. Nazar, *Angew. Chem., Int. Ed.* **2018**, *57*, 9795.

[66] J. Liu, Z. N. Bao, Y. Cui, E. J. Dufek, J. B. Goodenough, P. Khalifah, Q. Y. Li, B. Y. Liaw, P. Liu, A. Manthiram, Y. S. Meng, V. R. Subramanian, M. F. Toney, V. V. Viswanathan, M. S. Whittingham, J. Xiao, W. Xu, J. H. Yang, X. Q. Yang, J. G. Zhang, *Nat. Energy* **2019**, *4*, 180.

[67] P. Shi, X. B. Cheng, T. Li, R. Zhang, H. Liu, C. Yan, X. Q. Zhang, J. Q. Huang, Q. Zhang, *Adv. Mater.* **2019**, *31*, 1902785.

[68] T. Hamann, L. Zhang, Y. Gong, G. Godbey, J. Gritton, D. McOwen, G. Hitz, E. D. Wachsman, *Adv. Funct. Mater.* **2020**, *30*, 1910362.

[69] G. T. Hitz, D. W. McOwen, L. Zhang, Z. Ma, Z. Fu, Y. Wen, Y. Gong, J. Dai, T. R. Hamann, L. Hu, E. D. Wachsman, *Mater. Today* **2019**, *22*, 50.

[70] X.-B. Cheng, H.-J. Peng, J.-Q. Huang, R. Zhang, C.-Z. Zhao, Q. Zhang, *ACS Nano* **2015**, *9*, 6373.

[71] R. Zhang, X.-B. Cheng, C.-Z. Zhao, H.-J. Peng, J.-L. Shi, J.-Q. Huang, J. Wang, F. Wei, Q. Zhang, *Adv. Mater.* **2016**, *28*, 2155.

[72] F. Shen, F. Zhang, Y. Zheng, Z. Fan, Z. Li, Z. Sun, Y. Xuan, B. Zhao, Z. Lin, X. Gui, X. Han, Y. Cheng, C. Niu, *Energy Storage Mater.* **2018**, *13*, 323.

[73] G. Yang, Y. Li, Y. Tong, J. Qiu, S. Liu, S. Zhang, Z. Guan, B. Xu, Z. Wang, L. Chen, *Nano Lett.* **2019**, *19*, 494.

[74] J. Jeong, J. Chun, W.-G. Lim, W. B. Kim, C. Jo, J. Lee, *Nanoscale* **2020**, *12*, 11818.

[75] Q. Yun, Y.-B. He, W. Lv, Y. Zhao, B. Li, F. Kang, Q.-H. Yang, *Adv. Mater.* **2016**, *28*, 6932.

[76] H. Zhao, D. Lei, Y.-B. He, Y. Yuan, Q. Yun, B. Ni, W. Lv, B. Li, Q.-H. Yang, F. Kang, J. Lu, *Adv. Energy Mater.* **2018**, *8*, 1800266.

[77] L.-L. Lu, J. Ge, J.-N. Yang, S.-M. Chen, H.-B. Yao, F. Zhou, S.-H. Yu, *Nano Lett.* **2016**, *16*, 4431.

[78] L.-L. Lu, Y.-Y. Lu, Z.-J. Xiao, T.-W. Zhang, F. Zhou, T. Ma, Y. Ni, H.-B. Yao, S.-H. Yu, Y. Cui, *Adv. Mater.* **2018**, *30*, 1706745.

[79] C.-P. Yang, Y.-X. Yin, S.-F. Zhang, N.-W. Li, Y.-G. Guo, *Nat. Commun.* **2015**, *6*, 8058.

[80] P. Xue, S. Liu, X. Shi, C. Sun, C. Lai, Y. Zhou, D. Sui, Y. Chen, J. Liang, *Adv. Mater.* **2018**, *30*, 1804165.

[81] S. Liu, X. Xia, Y. Zhong, S. Deng, Z. Yao, L. Zhang, X.-B. Cheng, X. Wang, Q. Zhang, J. Tu, *Adv. Energy Mater.* **2018**, *8*, 1702322.

[82] L. Liu, Y.-X. Yin, J.-Y. Li, N.-W. Li, X.-X. Zeng, H. Ye, Y.-G. Guo, L.-J. Wan, *Joule* **2017**, *1*, 563.

[83] T.-T. Zuo, X.-W. Wu, C.-P. Yang, Y.-X. Yin, H. Ye, N.-W. Li, Y.-G. Guo, *Adv. Mater.* **2017**, *29*, 1700389.

[84] P. Shi, T. Li, R. Zhang, X. Shen, X.-B. Cheng, R. Xu, J.-Q. Huang, X.-R. Chen, H. Liu, Q. Zhang, *Adv. Mater.* **2019**, *31*, 1807131.

[85] H. Lee, J. Song, Y.-J. Kim, J.-K. Park, H.-T. Kim, *Sci. Rep.* **2016**, *6*, 30830.

[86] S.-H. Wang, Y.-X. Yin, T.-T. Zuo, W. Dong, J.-Y. Li, J.-L. Shi, C.-H. Zhang, N.-W. Li, C.-J. Li, Y.-G. Guo, *Adv. Mater.* **2017**, *29*, 1703729.

[87] D. Zhang, A. Dai, M. Wu, K. Shen, T. Xiao, G. Hou, J. Lu, Y. Tang, *ACS Energy Lett.* **2020**, *5*, 180.

[88] X. Yan, Q. Zhang, W. Xu, Q. Xie, P. Liu, Q. Chen, H. Zheng, L. Wang, Z.-Z. Zhu, D.-L. Peng, *J. Mater. Chem. A* **2020**, *8*, 1678.

[89] S.-H. Hong, D.-H. Jung, J.-H. Kim, Y.-H. Lee, S.-J. Cho, S. H. Joo, H.-W. Lee, K.-S. Lee, S.-Y. Lee, *Adv. Funct. Mater.* **2020**, *30*, 1908868.

[90] F. Pouraghajan, H. Knight, M. Wray, B. Mazzeo, R. Subbaraman, J. Christensen, D. Wheeler, *J. Electrochem. Soc.* **2018**, *165*, A2644.

[91] I. V. Thorat, D. E. Stephenson, N. A. Zacharias, K. Zaghib, J. N. Harb, D. R. Wheeler, *J. Power Sources* **2009**, *188*, 592.

[92] Y. Zhang, W. Luo, C. Wang, Y. Li, C. Chen, J. Song, J. Dai, E. M. Hitz, S. Xu, C. Yang, Y. Wang, L. Hu, *Proc. Natl. Acad. Sci.* **2017**, *114*, 3584.

[93] Y.-C. Yin, Z.-L. Yu, Z.-Y. Ma, T.-W. Zhang, Y.-Y. Lu, T. Ma, F. Zhou, H.-B. Yao, S.-H. Yu, *Natl. Sci. Rev.* **2018**, *6*, 247.

[94] H. Chen, A. Pei, J. Wan, D. Lin, R. Vilá, H. Wang, D. Mackanic, H.-G. Steinrück, W. Huang, Y. Li, A. Yang, J. Xie, Y. Wu, H. Wang, Y. Cui, *Joule* **2020**, *4*, 938.

[95] Y. He, X. Ren, Y. Xu, M. H. Engelhard, X. Li, J. Xiao, J. Liu, J. G. Zhang, W. Xu, C. Wang, *Nat. Nanotechnol.* **2019**, *14*, 1042.

[96] S. H. Yu, X. Huang, J. D. Brock, H. D. Abruna, *J. Am. Chem. Soc.* **2019**, *141*, 8441.

[97] K. H. Chen, K. N. Wood, E. Kazyak, W. S. LePage, A. L. Davis, A. J. Sanchez, N. P. Dasgupta, *J. Mater. Chem. A* **2017**, *5*, 11671.

[98] X. Shen, R. Zhang, X. Chen, X. B. Cheng, X. Y. Li, Q. Zhang, *Adv. Energy Mater.* **2020**, *10*, 1903645.

[99] R. Zhang, X. Shen, X. B. Cheng, Q. Zhang, *Energy Storage Mater.* **2019**, *23*, 556.

[100] Q. Li, S. Zhu, Y. Lu, *Adv. Funct. Mater.* **2017**, *27*, 1606422.

[101] A. Zhang, X. Fang, C. Shen, Y. Liu, C. Zhou, *Nano Res.* **2016**, *9*, 3428.

[102] G. J. H. Lim, Z. Lyu, X. Zhang, J. J. Koh, Y. Zhang, C. He, S. Adams, J. Wang, J. Ding, *J. Mater. Chem. A* **2020**, *8*, 9058.

[103] Z. Lyu, G. J. H. Lim, R. Guo, Z. Pan, X. Zhang, H. Zhang, Z. He, S. Adams, W. Chen, J. Ding, J. Wang, *Energy Storage Mater.* **2020**, *24*, 336.
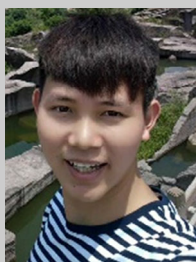
Ying-Xin Zhan obtained his M.S. from Wenzhou University in 2019. Currently, he is a Ph.D. student under the supervision of Professor Jia-Qi Huang at the School of Materials Science and Engineering, Beijing Institute of Technology. His research interests focus on energy storage materials, especially Li metal anodes.

Peng Shi obtained his B.S. from Beijing University of Chemical Technology in 2017. Currently, he is a Ph.D. student under the supervision of Professor Qiang Zhang at the Department of Chemical Engineering, Tsinghua University. His research interests focus on energy storage materials, especially Li metal anodes.

**ADVANCED
SCIENCE NEWS**

www.advancedsciencenews.com

Energy Technology
Generation, Conversion, Storage, Distribution

www.entechnol.de

Xue-Qiang Zhang obtained his B.S. degree from Tianjin University in 2016. He is currently a Ph.D. candidate at the Department of Chemical Engineering, Tsinghua University. His research interests focus on Li metal batteries, especially the interface between Li and an electrolyte and the solvation of Li ions in electrolytes.

Jia-Qi Huang received his B. Eng. (2007) and Ph.D. (2012) degrees in chemical engineering from Tsinghua University, China. He is currently a professor at the Advanced Research Institute of Multidisciplinary Science (ARIMS) in the Beijing Institute of Technology. His research interests focus on the interface phenomenon and design strategies for high-energy-density rechargeable batteries, including Li–S batteries and Li metal batteries.

Qiang Zhang received his bachelor's and Ph.D. degree from Tsinghua University in 2004 and 2009, respectively. After a stay in Case Western Reserve University, USA, and Fritz Haber Institute of the Max Planck Society, Germany, he was appointed as an associate professor in Tsinghua University in 2011. He was promoted to a full professor in 2017. His current interests focus on energy materials, including Li–S batteries, Li metal anodes, and electrocatalysts.